Inorg. Chem. **2003**, *42*, 4409–4416

Structure and Magnetic Properties of Layered High-Spin Co(II)(L-threonine)$_2$(H$_2$O)$_2$

Alberto C. Rizzi,[†] Carlos D. Brondino,[†] Rafael Calvo,*[,†] Ricardo Baggio,[‡] María T. Garland,[§] and Raul E. Rapp[||]

Departamento de Física, Facultad de Bioquímica y Ciencias Biológicas, Universidad Nacional del Litoral and INTEC (CONICET-UNL), Güemes 3450, 3000 Santa Fe, Argentina, Departamento de Física, Comisión Nacional de Energía Atómica, Avda. del Libertador 8250, 1429 Buenos Aires, Argentina, Departamento de Física, Facultad de Ciencias Físicas y Matemáticas, Universidad de Chile, Avda. Blanco Encalada 2008, Casilla 487-3, Santiago, Chile, and Instituto de Física, Universidade Federal do Rio de Janeiro, CP 68528, Rio de Janeiro 21945, RJ, Brazil

Received October 16, 2002

We report the structure and the magnetic properties of a cobalt(II) compound with the amino acid L-threonine, Co(C$_4$H$_8$NO$_3$)$_2$(H$_2$O)$_2$. It crystallizes in the orthorhombic chiral space group $C222_1$, with $a = 5.843(5)$ Å, $b = 10.120(10)$ Å, $c = 22.36(3)$ Å, and $Z = 4$. The Co(II) ion is in a deformed octahedral environment on a 2-fold symmetry axis parallel to the crystallographic axis *b*. It is bonded to two threonine molecules in a bidentate fashion, via one oxygen from the carboxylate end and the α-amino nitrogen. A water molecule occupies the third independent site. The Co(II) ions are arranged in layers with intralayer and interlayer distances of 5.84 and 11.18 Å, respectively. Magnetic measurements data reflect the molecular character of a compound with weak exchange interactions. EPR measurements in polycrystalline and single-crystal samples indicate a distorted axial symmetry around the Co(II) ion, as expected from the structural results. Eigenvalues and eigenvectors of the **g** tensor are determined. The measured principal *g* values (5.81, 4.56, and 2.23) reflect a high-spin Co(II) ion, as suggested by the type of ligands and the molecular symmetry. From the incomplete collapse of the hyperfine structure we estimate $0.25 < |J| < 1.2$ cm^{-1} between neighboring Co(II) ions within a layer, transmitted through H-bonds. A higher limit $|J'| < 0.07$ cm^{-1} is estimated for the exchange interactions between Co(II) ions in neighboring layers. From a global fit of a spin Hamiltonian with spin $^3/_2$ to magnetization and EPR data we obtain a zero field splitting $\delta \sim 231$ cm^{-1} between the two lowest doublet states. The results are discussed in terms of the molecular and electronic structure of the compound.

Introduction

Despite its low availability in the earth's crust,[1] cobalt plays important roles in biological systems. The most common examples are vitamin B$_{12}$ and coenzyme B$_{12}$, a cofactor required for a group of enzymatic systems of central importance in biochemistry.[2] Furthermore, several cobalt-containing metalloproteins with the metal ion bonded to amino acid residues have been characterized.[3−5] Because of its high sensitivity to the coordination site geometry and the many experimental techniques that can be used in its characterization, cobalt has been used to substitute for other metal ions to gather information about changes in metal sites in proteins during protein function.[6−9] Spectroscopic characterization of these systems has revealed that cobalt can be

* Author to whom correspondence should be addressed. E-mail: rcalvo@dfbioq.unl.edu.ar.
[†] Universidad Nacional del Litoral and INTEC.
[‡] Comisión Nacional de Energía Atómica.
[§] Universidad de Chile.
[||] Universidade Federal do Rio de Janeiro.

(1) Lippard, S. J.; Berg, J. M. *Principles of Bioinorganic Chemistry*; University Science Books: Mill Valley, CA, 1994.
(2) Fraústo da Silva, J. J. R.; Williams, R. J. P. *The Biological Chemistry of the Elements*; Clarendon Press: Oxford, 1997.
(3) Rulísek, L.; Vondrasek, J. *J. Inorg. Biochem.* **1998**, *71*, 115−127.
(4) Payne, M. S.; Wu, S.; Fallon, R. D.; Tudor, G.; Stieglitz, B.; Turner, I.; Nelson, M. *Biochemistry* **1997**, *36*, 5447−5454.
(5) Gavel, O. Y.; Bursakov, S. A.; Calvete, J. J.; George, G. N.; Moura, J. J.; Moura, I. *Biochemistry* **1998**, *46*, 16225−16232.
(6) Carvalho, E.; Aasa, R.; Göthe, P. *J. Inorg. Biochem.* **1996**, *62*, 147−153.
(7) Bonander, N.; Vänngard, T.; Tsai, L.; Langer, V.; Nar, H.; Sjölin, L. *Proteins* **1997**, *27*, 385−394.

10.1021/ic026111b CCC: $25.00
Published on Web 05/28/2003

present as Co(II) and Co(III) ions in several types of coordination, which lead to different electronic and magnetic properties. In this context, the use of simple Co-containing systems with low molecular weight ligands is useful for understanding the correlation between magnetic and structural properties.

Structures of cobalt complexes with the amino acids glutamic and aspartic acid,[10,11] histidine,[12] glycine,[13,14] phenylalanine,[15] alanine,[16] methionine,[11] *S*-methyl-cysteine,[11] and asparagine[17] have been reported.[18,19] Less information exists about the electronic and magnetic properties of cobalt-amino acid compounds, although amino acid compounds of a simpler metal like copper have received much more attention. This is because Co(II) and Co(III) ions have the more complex $3d^7$ and $3d^6$ ground configurations, respectively, with the higher complications introduced by the orbital and spin degeneracy of the ground state. In the case of Co(II) ion in an octahedral environment, the ^4F ground term splits into two orbital triplets ($^4T_{1g}$ and $^4T_{2g}$) and one orbital singlet ($^4A_{2g}$), $^4T_{1g}$ being the ground-state multiplet. This is further split by the spin−orbit interaction and by lower symmetry distortions of the ligand field, thus producing a wide variety of magnetic behaviors, which strongly depend on the details of the molecular structure and the resulting energy level scheme.[20,21] Kahn[21] discusses models to analyze the magnetic properties of Co(II) compounds in octahedral coordination with axial distortion. High-spin ($S = {}^3/_2$) or low-spin ($S = {}^1/_2$) is a basic classification of Co(II) compounds depending on the magnitudes of the energy gap between the metal orbitals relative to the mean spin pairing energy.[21] Magnetic characterization of these compounds provide information about the electronic structure of single cobalt ions and also about the interactions between them. The exchange interactions (defined as $\sum_{i>j} - J_{ij}\mathbf{S}_i\cdot\mathbf{S}_j$), which are transmitted through the weak bonds that provide the paths for superexchange typical of amino acid and protein structures, can be evaluated.

We report herein the structure and the magnetic properties of a Co(II) ion compound with the amino acid L-threonine, $Co(C_4H_8NO_3)_2(H_2O)_2$, to be called Co(L-Thr)$_2$. Its structure was solved by X-ray techniques and its electronic properties and magnetic interactions have been studied by EPR and magnetic measurements.

Experimental Section

Materials and Methods. All chemicals, of commercially available reagent grade, were used as received. Water was purified by a Millipore Milli-Q system, yielding 18 MΩ-cm water. Elemental analyses (C, H, N) were performed on a Carlo Erba EA 1108 analyzer. Infrared spectra were recorded as KBr disks and as a mull in Nujol with a Nicolet 510 FT-IR spectrophotometer. The electronic spectrum in the solid was recorded in the 200−800-nm range on a Shimadzu 3101 PC spectrophotometer equipped with an integrating sphere. Powder X-ray diffraction (XRD) data were collected using monochromated Cu Kα radiation on a Phillips X'Pert diffractometer. Single-crystal XRD data were collected on a Siemens *R*3*m* diffractometer using Mo Kα radiation (λ = 0.71069Å). Magnetic data were obtained with a Quantum Design PPMS magnetometer. X-band CW EPR spectra were obtained at 4 K on a Bruker ER-200 spectrometer, equipped with an Oxford Instrument helium continuous-flow cryostat and a rectangular cavity with 100 kHz field modulation. Powder sample for EPR and magnetic measurements were obtained grinding single crystals.

Preparation of [Co(L-threonine)$_2$(H$_2$O)$_2$]. Cobalt carbonate (Alfa Aesar, >99%, 0.1190 g, 1 mmol) was added to 10 mL of a water solution of L-threonine (Sigma Ultra, >99% TLC, 0.2382 g, 2 mmol). The mixture was stirred for a few minutes at room temperature until an intense red color developed, and then it was passed through a 0.22-μm Millipore filter. The filtrate was stored and well-shaped pink hexagonal (001) plates, having dimensions up to about 1 × 1 × 0.5 mm, were separated by filtration after several days, washed with cold water, and dried in air. Equal result is obtained using Co(II) acetate tetrahydrate, raising carefully the pH of the solution to 6.2 with 1 M NaOH. The positions of the *a* and *b* crystal axes were identified with a goniometric microscope. Yield: 0.10 g, 35%. A powder X-ray diffraction pattern of the bulk sample compared well with the pattern simulated from the single-crystal data. Anal. Calcd for $C_8H_{20}N_2O_8Co$: C, 29.0; H, 6.1; N, 8.5. Found: C, 29.1; H, 6.3; N, 8.5. FT-IR (KBr disk, cm^{-1}): 3306 vs; 3253 vs, br; 2972 vs; 2938 m; 1614 vs; 1586 vs ($\nu(COO^-)_{asym}$); 1444 m; 1404 vs ($\nu(COO^-)_{sym}$); 1365 s; 1342 w; 1153 s; 1132 s; 1087 m; 1040 vs; 1002 m; 899 m; 802 m; 686 m; 635 m; 579 m; 537 w; 473 w. UV−vis (solid): band at 495 nm ($^4T_{1g}(F) \rightarrow {}^4T_{1g}(P)$, where the $^4T_{1g}$ orbital triplets are split by the low-symmetry components of the crystal field).[22]

Single-Crystal Diffraction Data and Structure Solution and Refinement. Crystal data for the complex Co(L-Thr)$_2$ are summarized in Table 1. Further details on the data collection procedures, structural determination methods, and structure refinement are given as Supporting Information. The structures were solved by direct methods (SHELXS-97)[23] and refined by full-matrix least-squares on F^2 (SHELXL-97).[24] Hydrogen atoms relevant for the description of the H-bonding (O−H's and N−H's) were found in a late

(8) Adrait, A.; Jacquamet, L.; Le Pape, L.; Gonzalez de Peredo, A.; Aberdam, D.; Hazemann, J. L.; Latour, J. M.; Michaud-Soret, I. *Biochemistry* **1999**, *38*, 6248−6260.
(9) Strand, K. R.; Karlsen, S.; Andersson, K. K. *J. Biol. Chem.* **2002**, *277*, 34229−34238.
(10) Doyne, T.; Pepinsky, R. *Acta Crystallogr.* **1957**, *10*, 438−439. Pepinsky, R.; Turley, J. W.; Okaya, Y.; Doyne, T.; Vand, V.; Shimada, A.; Lovell, F. M.; Sogo, Y. *Acta Crystallogr.* **1957**, *10*, 811−812.
(11) Isago, T.; Igi, K.; Hidaja, J. *Bull. Chem. Soc. Jpn.* **1979**, *52*, 407−414.
(12) Harding, M. M.; Long, H. A. *J. Chem. Soc. (A)* **1968**, 2554−2559. Candlin, R.; Harding, M. M. *J. Chem. Soc. (A)* **1970**, 384−393.
(13) Clegg, W.; Lacy, O. L.; Straughan, B. P. *Acta Crystallogr. C* **1987**, *43*, 794−797.
(14) Ravikumar, K.; Rajan, S. S. *Z. Kristallogr.* **1985**, *171*, 201−207.
(15) Demaret, A.; Abello, L.; Fourati, M.; Lapluye, G. *J. Chem. Res. (S)* **1978**, 354−355.
(16) Herak, R.; Prelesnik, B.; Krstanovic, I. *Acta Crystallogr. B* **1978**, *34*, 91−95.
(17) Sekisaki, M. *Bull. Chem. Soc. Jpn.* **1979**, *52*, 403−406.
(18) Allen, F. H. *Acta Crystallogr.* **2002**, *B58*, 380−388.
(19) Bruno, I. J.; Cole, J. C.; Edington, P. R.; Kessler, M.; Macrae, C. F.; McCabe, P.; Pearson, J.; Taylor, R. *Acta Crystallogr.* **2002**, *B58*, 389−397.
(20) Abragam, A.; Bleaney, B. *Electron Paramagnetic Resonance of Transition Ions*; Clarendon Press: Oxford, 1970.
(21) Kahn, O. *Molecular Magnetism*; VCH: New York, 1993.
(22) Drago, R. S. *Physical Methods for Chemists*; Saunders College Publishing: Philadelphia, 1992.
(23) Sheldrick, G. M. *SHELXS−97. Program for Structure Resolution*; University of Göttingen: Göttingen, Germany, 1997.
(24) Sheldrick, G. M. *SHELXL−97. Program for Structure Refinement*. University of Göttingen: Göttingen, Germany, 1997.

Table 1. Crystallographic Data for Co(L-Thr)$_2$

formula	$CoC_8H_{20}N_2O_8$
fw	331.19
cryst syst/space group	orthorhombic/$C222_1$
a, Å	5.843(5)
b, Å	10.120(10)
c, Å	22.36(3)
cell vol, Å^3	1322(3)
formula units/unit cell	4
ρ_{calc}, g cm^{-3}	1.664
μ_{calc}, cm^{-1}	1.335
T, K	293
$R = \Sigma\|\|F_o\| - \|F_c\|\|/\Sigma\|F_o\|$	0.052
wR2 = $[\Sigma[w(F_o^2 - Fc^2)^2]/\Sigma[w(F_o^2)^2]]^{1/2}$	0.109

difference Fourier synthesis and refined with constrained O−H/N−H distances; those attached to carbon were positioned theoretically and allowed to ride. A complete set of the results of the XRD crystallographic structural data has been deposited at the Cambridge Structural Database (CSD) in CIF format (deposition number CCDC 206359).

Magnetic Measurements. Magnetization measurements were performed in a powder sample of 44.5(1) mg of Co(L-Thr)$_2$ as a function of temperature (T) for various fixed values of the static dc magnetic field between 0.03 and 90 kG and at fixed temperatures $T = 2$, 4, and 10 K as a function of the applied magnetic field. The molar dc static susceptibility $\chi_M(T)$ was calculated from magnetization data obtained with a field of 1 kG. All data presented in this work were corrected for the diamagnetic contribution ($\chi_D = -1.48 \times 10^{-4}$ emu/mol) calculated using Pascal constants.[21,25]

EPR Measurements. X-band CW EPR spectra of powder and single-crystal samples of Co(L-Thr)$_2$ were obtained at 4 K. The EPR parameters were obtained from spectral simulations of a powder sample using the program SimFonia (v. 1.25, Bruker Instruments Inc.).

The sample for the single-crystal EPR measurements was oriented by gluing the (001) face of a hexagonal single-crystal plate to a cleaved KCl cubic holder, which defines a set of orthogonal laboratory axes $x_Ly_Lz_L$. Thus, the c crystal direction is along the z_L axis, and a (110) lateral face of the single crystal was positioned perpendicular to the x_L axis. This sample holder was introduced into a 4-mm o.d. quartz tube and positioned in the center of the microwave cavity. The tubes were attached to a goniometer and the sample was rotated in steps of 10° with the magnetic field in the planes x_Ly_L, z_Ly_L, and x_Lz_L of the sample holder.

A Global Fitting Procedure: Simulated Annealing. Along this work we used the simulated annealing method[26] to perform a global fit of the parameters of a model to experimental data obtained from different experimental techniques (magnetization and EPR measurements). The use of this method for fitting experimental results has been described previously.[27,28]

Experimental Results and Analysis

The reaction of Co(II) carbonate with L-threonine in the mole ratio 1:2 in water at room temperature and subsequent workup led to the isolation of pink crystals of Co(L-Thr)$_2$. Elemental analyses, IR and UV−vis spectra, and powder XRD data supported the formulation of the compound. The solid compound is stable when kept in a dry atmosphere and is slightly soluble in polar and nonpolar solvents.

Crystal and Molecular Structure of Co(L-Thr)$_2$. The compound crystallizes in the orthorhombic chiral space group $C222_1$, with four monomeric units per unit cell. Selected bond distances and angles and hydrogen-bonding parameters are given in Table 2. Fractional coordinates and equivalent isotropic temperature parameters for Co(L-Thr)$_2$ are given in additional tables included as Supporting Information.

The Co(II) ion is in a deformed octahedral environment on a 2-fold symmetry axis parallel to the crystallographic b axis. It is bonded in a bidentate fashion to two threonine molecules, via one carboxylate oxygen and the α-amino nitrogen (see Figure 1). A water molecule occupies the third independent position. The rest of the coordination sphere is generated by the 2-fold axis bisecting the group through the cation.

Coordination distances are quite even (Co−N1: 2.133(7) Å, Co−O1: 2.103(6) Å, Co−O1w: 2.090(6) Å). The slightly longer N1−Co1−N1′ line shows the smallest distortion from a straight line, and it is approximately perpendicular to the b symmetry axis. The deformed perpendicular plane of the octahedron is fully occupied by oxygen atoms, with a mean deviation from the best plane of 0.24 Å. The octahedral coordination and the type of ligands suggest high-spin Co(II) magnetic behavior.

In Co(L-Thr)$_2$, there are four chemically equivalent Co molecules in the unit cell, which are related by the symmetry operations of the space group $C222_1$ (Figure 2a). Co1, at the special position $(0,y,{}^1/_4)$, is related to Co3 by a translation $({}^1/_2,{}^1/_2,0)$, as well as Co2 to Co4. Co1 is related to Co2, at the special position $(0,-y,{}^3/_4)$, by a C_{2c} rotation plus a translation $(0,0,{}^1/_2)$, as well as Co3 to Co4. Neighboring monomeric units interact with each other via H-bonding to form 2D structures normal to the c axis, with cobalt layers at $z = c/4$ and $z = 3c/4$ separated by $c/2 = 11.18$ Å (Figure 2b). Equally oriented (obtained by translations) Co1 and Co3 molecules are in one layer, whereas Co2 and Co4 molecules, with the other orientation, are in the neighboring layer. Therefore, from the magnetic point of view, the compound can be assumed as having two magnetically nonequivalent molecules per unit cell, a result which is important in the analysis of the EPR spectra. The H-bond O1···H1wb−O1w provides the shortest and most important Co−Co interaction, connecting a cobalt ion with four cobalt neighbors within the layer (see Figure S1 in Supporting Information). These bonds are quite linear, 168°, and short, $d_{D-A} = 2.84$ Å (see Table 2). Other H-bonds connecting Co(II) ions translated $\pm a$ within the layer are tortuous and involve nine atoms between them.

The coordination of the Co(II) ion in Co(L-Thr)$_2$ is similar to that reported for the Zn(II) ion in Zn(L-threonine)$_2$(H$_2$O)$_2$ [29] and different from that of the Cu(II) ion in Cu(II)(L-

(25) Carlin, R. *Magnetochemistry*; Springer: Berlin, 1986.
(26) Kirpatrick, S.; Gelatt, C. D.; Vecchi, M. P. *Science* **1983**, *220*, 671−680.
(27) Calvo, R.; Abresch, E. C.; Bittl, R.; Feher, G.; Hofbauer, W.; Isaacson, R. A.; Lubitz, W.; Okamura, M. Y.; Paddock, M. L. *J. Am. Chem. Soc.* **2000**, *122*, 7327−7341.
(28) Calvo, R.; Passeggi, M. C. G.; Moreno, N. O.; Barberis, G. E.; Braun Chaves, A.; Torres, B. C. M.; Lezama, L.; Rojo, T. *Phys. Rev. B* **1999**, *60*, 1197−1203.
(29) Hämäläinen, R. *Finn. Chem. Lett.* **1977**, 113−117.

Table 2. Selected Interatomic Bond Distances (Å) and Angles (deg) for Co(L-Thr)$_2$, Including Hydrogen Bonds[a]

Bond Lengths

Co(1)−O(1W)	2.090(6)	Co(1)−O(1)	2.103(6)	Co(1)−N(1)	2.133(7)

Bond Angles

O(1W)−Co(1)−O(1)#1	166.3(2)	O(1W)−Co(1)−N(1)	96.2(3)
N(1)−Co(1)−N(1)#1	173.6(4)	O(1W)#1−Co(1)−N(1)	88.1(3)
O(1W)−Co(1)−O(1W)#1	93.8(4)	O(1)−Co(1)−N(1)#1	96.7(3)
O(1)#1−Co(1)−O(1)	87.4(3)	O(1)−Co(1)−N(1)	78.6(2)
O(1W)−Co(1)−O(1)	90.9(3)		

Hydrogen Bond Distances and Angles

D	H	A	D···A	H···A	⟨D−H···A	D−H
O3	H3	O2#2	2.69(1)	1.96(9)	167(7)	0.73(9)
N1	H1B	O2#3	3.05(1)	2.17(7)	171(7)	0.88(7)
O1W	H1WA	O3#4	2.71(1)	1.85(7)	157(6)	0.90(6)
O1W	H1WB	O1#5	2.84(1)	1.95(7)	168(7)	0.89(7)

[a] D and A indicate donor and acceptor atoms, respectively. Symmetry transformations used to generate equivalent atoms: #1, $-x-2, y, -z+{}^1/_2$; #2, $x-1, y, z$; #3, $x-{}^1/_2, y+{}^1/_2, z$; #4, $x+{}^1/_2, y+{}^1/_2, z$; #5, $-x-{}^3/_2, y+{}^1/_2, -z+{}^1/_2$.

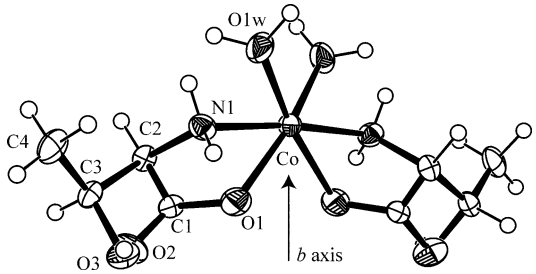

Figure 1. Ellipsoid plot of Co(L-Thr)$_2$ showing the atoms labeling and the coordination sphere around the Co(II) ion. The C_2 symmetry axis parallel to the *b* axis of the Co(II) site is indicated.

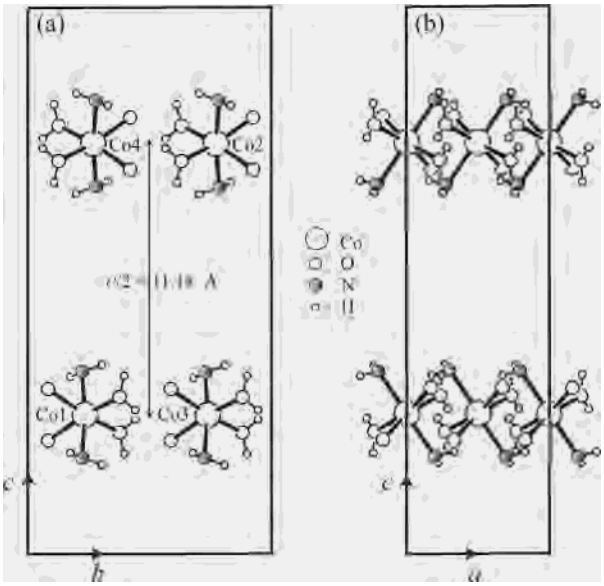

Figure 2. (a) Projection along *a* of the four cobalt ions and their ligands in the unit cell. The distance between cobalt layers is also indicated. (b) Structure of the cobalt layers, projected along *b*.

threonine)$_2$·H$_2$O.[30] In this last compound, the Cu(II) ion is equatorially bonded to one carboxylic oxygen and one amino nitrogen of two threonine molecules, whereas the axial positions are occupied by carboxylic oxygen of other two threonine molecules. The carboxylate group acts as an equatorial-apical bridge connecting copper molecules and

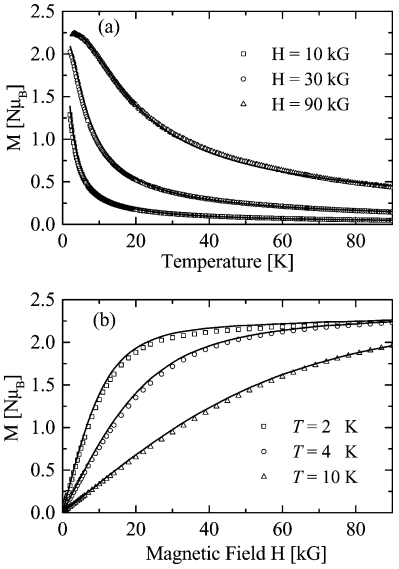

Figure 3. Molar magnetization in Nμ_B units of a powder sample of Co(L-Thr)$_2$ measured (a) as a function of temperature for three values of magnetic field and (b) as a function of magnetic field at three temperatures. The solid lines were obtained by global fitting eq 3 to the magnetic and EPR data.

provides the shortest chemical path between Cu(II) ions. In the cobalt compound studied here this role is played by H-bonds, and thus the Co(L-Thr)$_2$ molecules are expected to be more independent than the Cu(L-Thr)$_2$ molecules. For the zinc compound, the Zn(II) ions are coordinated through the α-amino nitrogen and the carboxylic oxygen with two water molecules completing the octahedral coordination, as in the cobalt compound. However, the Zn(II) site has no C_2 symmetry axis through the metal ion. Both Zn(L-threonine)$_2$(H$_2$O)$_2$ and Co(L-threonine)$_2$(H$_2$O)$_2$ have the amino acid groups in cis positions whereas the copper compound has them in the trans position.

dc Magnetization Measurements. The dc molar magnetization *M* of a powder sample of Co(L-Thr)$_2$ was measured as a function of temperature, *T*, between 2.0 and 90 K, for several values of the applied magnetic field *H* (Figure 3a). A magnetization saturation $M_{sat}/(N\mu_B) = 2.19$ is approached at high magnetic fields and low temperatures. The magnetization was also measured as a function of H at 2, 4, and

(30) Rizzi, A. C.; Piro, O. E.; Castellano, E. E.; Nascimento, O. R.; Brondino, C. D *Inorg. Chim. Acta* **2000**, *305*, 19−25.

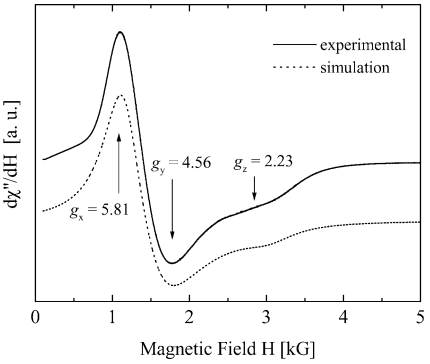

Figure 4. EPR spectra of a powder sample of Co(L-Thr)$_2$ obtained at 9.475 GHz and $T = 4$ K. Simulation and principal values of the molecular **g** tensor are included.

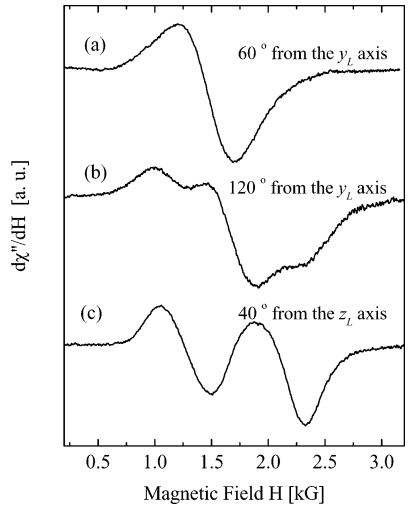

Figure 5. EPR spectra obtained for some representative directions of the magnetic field at 9.475 GHz and $T = 4$ K for a single crystal of Co(L-Thr)$_2$. (a) and (b) x_Ly_L plane. (c) z_Lx_L plane.

10 K (Figure 3b). M still increases at the highest fields, and the saturation situation is not readily reached, even at 2 K (see Figure 3b). No differences were observed between $M(H)$ curves measured with increasing or decreasing magnetic field.

EPR Measurements. The X-band EPR spectrum of a polycrystalline sample of Co(L-Thr)$_2$ at 4 K is shown in Figure 4. The peaks broaden at higher T and disappear at ~50 K. This spectrum can be assigned to transitions between the states of a spin doublet having a highly anisotropic g-factor. The hyperfine structure expected for the 100% abundant ^{59}Co isotope ($^{59}I = {}^7/_2$) is not observed in the spectrum of the powder sample.

Single-crystal EPR spectra were recorded with the magnetic field in the x_Ly_L, z_Lx_L, and z_Ly_L planes; Figure 5 shows selected spectra obtained in the x_Ly_L and z_Lx_L planes. Since the two Co(II) ions are related by a C_2 rotation around the $c = z_L$ axis, they are magnetically equivalent for the magnetic field applied in the $ab = x_Ly_L$ plane and along the c axis. They are magnetically nonequivalent for magnetic fields applied in any other direction. In the absence of exchange interactions between Co(II) ions one expects one resonance pattern with eight hyperfine components for any magnetic field orientation in the x_Ly_L plane and along the c axis and two patterns of hyperfine components in other directions. When the magnitude of the exchange interaction J between neighboring Co(II) ions in the same layer is larger than the magnitude of the hyperfine coupling parameter A ($|J| > |A|$), the hyperfine structure collapses and gives a single collapsed peak. This was shown by Farach et al.[31] for ${}^1/_2 \leq I \leq {}^5/_2$ (see also refs 32 and 33). In this work we verified that the case for $I = {}^7/_2$ follows the same trend observed by Farach et al. for smaller I. As explained before for a general case,[34] and considering the layered structure of Co(L-Thr)$_2$, the possible collapse of the resonances corresponding to the two rotated Co(II) ions is related to the magnitude of the smaller exchange interactions between Co(II) ions in neighboring layers, J'. These resonances collapse when the difference between their Zeeman energies, $\Delta g\mu_B H$, is smaller than $|J'|$ (Δg is the difference between the g-factors for the two Co(II) sites for a given direction of the magnetic field H and μ_B is the Bohr magneton). Thus, EPR data provides information about the absolute values of both, the intralayer interaction J (from the collapse of the hyperfine structure), and the interlayer interaction J'(from the collapse of the resonances corresponding to the two rotated Co(II) ions).

In the *ab* plane we observe one resonance line with Lorentzian line shape for some magnetic field orientations (Figure 5a) and a central line with two lateral lines for other orientations (Figure 5b). Thus, in the former case the exchange interaction J between Co(II) ions is large enough to collapse the eight hyperfine components to a single line, whereas in the latter case, J collapses only the six central hyperfine lines ($|J| > |A|$).[31] We attribute this behavior to the angular dependence of A:[20] $|A|$ is smaller or larger than $|J|$ for different magnetic field orientations and the collapse condition changes with angle. From the observed incomplete collapse of the hyperfine structure and following the theory described by Farach et al.[31] (and our own calculations for the case $I = {}^7/_2$) we estimated $0.25 < |J| < 1.2$ cm^{-1} between neighboring Co(II) ions within a layer transmitted through H-bonds. A value $|A| \sim 100$ G, typical for octahedral high-spin Co(II) ions,[35,36] was assumed for the estimation of J. The collapse of the hyperfine structure produces the observed Lorentzian line shape.

In the z_Lx_L plane we observe two resonances with equal intensities, showing no hyperfine structure (Figure 5c). These resonances have symmetry-related angular variations and are assigned to the two rotated Co(II) ions in the unit cell. In the z_Ly_L plane the observed spectra (not shown) are a superposition of the resonances expected for the two rotated Co(II) ions, having each line lateral hyperfine components, as observed in the x_Ly_L plane (see above). The complexity of the spectra in the z_Ly_L plane prevents a detailed analysis.

(31) Farach, H.; Strother, E. F.; Poole, C. P. *J. Phys. Chem. Solids* **1970**, *31*, 1491−1510.
(32) Calvo, R.; Isern, H.; Mesa, M. A. *Chem. Phys.* **1985**, *100*, 89−99.
(33) Brondino, C. D.; Calvo, R.; Baran, E. J. *Chem. Phys. Lett.* **1997**, *271*, 51−54.
(34) Passeggi, M. C. G.; Calvo, R. *J. Magn. Reson. A* **1995**, *114*, 1−11.
(35) Goñi, A.; Lezama, L. M.; Rojo, T.; Foglio, M. E.; Valdivia, J. A.; Barberis, G. E. *Phys. Rev. B* **1998**, *57*, 246−251.
(36) Pilbrow, J. R. *Transition Ion Electron Paramagnetic Resonance*; Oxford University Press: New York, 1990.

Table 3. Principal Values g_x, g_y, and g_z of the **g** Tensor Corresponding to the Ground Doublet of Co(II) Ion Obtained from the EPR Spectrum of a Powder Sample

eigenvalues	eigenvectors[a]	angles
$g_x = 5.81(2)$	a_x, $a_x^* = [\mp 0.408, 0, 0.913]$	a_x−(Co−N) = 10.5°
$g_y = 4.56(2)$	a_y, $a_y^* = [0, \pm 1, 0]$	
$g_z = 2.23(2)$	a_z, $a_z^* = [\pm 0.913, 0, 0.408]$	a_z^*−(Co−N) = 31.9°

[a] Eigenvectors a_x, a_y, and a_z and a_x^*, a_y^*, and a_z^* of the **g** tensor for the two rotated Co(II) ions in the unit cell are given in the *abc* axes system. Some angles between eigenvectors and the Co−N bond are also included.

However, we observe that the magnitude $|J'|$ of the exchange interaction between Co(II) ions in neighboring layers is not large enough to collapse the resonances corresponding to the two cobalt sites in the unit cell.

Figure 6a,b shows the angular variation of the *g* factor as a function of the angle α with the y_L axis in the x_Ly_L plane (defined in the inset) and β with the z_L axis in the z_Lx_L plane. The symmetry of the angular variation of the EPR spectra confirms the assignment of the crystal axes of the sample described in the Experimental Section. Since the EPR transitions occur only within the ground Kramers' doublet, we assume a spin Hamiltonian with an effective spin $S' = {}^1/_2$:

$$\mathcal{H} = \mu_B \mathbf{S'} \cdot \mathbf{g} \cdot \mathbf{H} \qquad (1)$$

Under this spin Hamiltonian the excited doublet of the $S = {}^3/_2$ multiplet (not considered in eq 1) is responsible for the large anisotropy observed for the *g*-value of the ground doublet. Information about the Co(II) ions is contained in the eigenvalues and eigenvectors of the **g** tensor. We obtained the eigenvalues $g_x = 5.81$, $g_y = 4.56$, and $g_z = 2.23$ from simulation of the powder spectrum assuming Lorentzian line shapes, and angular variation of the line width having common principal axes with the **g** tensor. The rhombic symmetry of the **g** tensor is supported by the distorted octahedral coordination of the Co(II) ion in Co(L-Thr)$_2$; the observed large *g* anisotropy is typical of high-spin Co(II) compounds.[20,37] To evaluate the eigenvectors of the **g** tensor, we used the single-crystal results and the eigenvalues obtained from the spectrum of the powder sample (see Table 3 and Figure 4). From the angular variation of the *g* factor measured on the x_Ly_L plane we obtained $g = 4.56$ along the *b* axis. This value agrees with one eigenvalue obtained from the powder sample. This result is expected since *b* is a C_2 symmetry axis of the Co(II) ion site and, consequently, an eigenvector of the molecular **g** tensor. The eigenvectors corresponding to the other two eigenvalues, which are contained in the *ac* plane, were calculated using the single-crystal EPR results in the x_Ly_L and z_Lx_L planes and the eigenvalues provided by the EPR powder data. The results are given in Table 3. Since the unit cell contains two rotated molecules, there are two possible orientations for the principal axes of the **g** tensor in the molecular frame (see Discussion). The solid lines in Figure 6a,b, obtained using the values in Table 3, are in good agreement with the experiments. The differences observed for some orientations

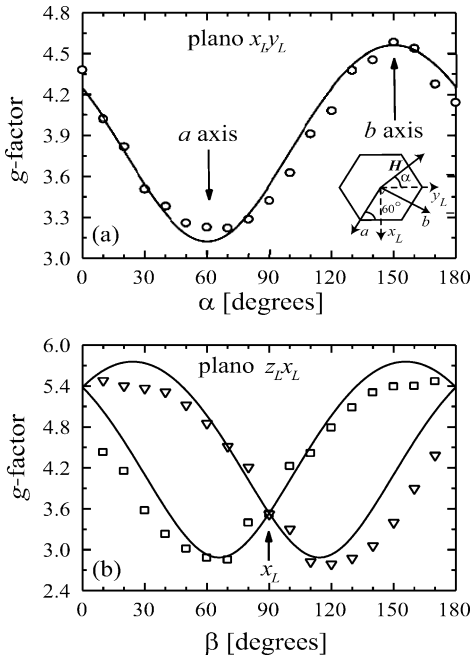

Figure 6. Angular variation of the *g* factor of Co(L-Thr)$_2$ obtained at 9.475 GHz and $T = 4$ K for a single crystal of Co(L-Thr)$_2$. (a) x_Ly_L plane. (b) z_Lx_L plane; squares and triangles indicate the position of the two resonance lines for this plane. The solid lines in both plots correspond to the angular variation of the EPR line position, calculated with the components of the molecular $\mathbf{g}^2$ tensor.

are attributed to the uncertainties in the fitting of the line positions which arise from the overlap and the large width of the resonances.

The fact that two EPR lines are observed in the z_Lx_L and in the z_Ly_L planes indicates that the interlayer exchange interaction J' is not large enough to collapse the resonances of the two magnetically nonequivalent Co(II) ions, allowing us to estimate $|J'| < \Delta g \mu_B H \sim 0.07$ cm^{-1} between Co(II) ions in neighboring layers ($\Delta g \sim 1$ estimated at 10° from the z_L axis in the z_Lx_L plane, see Figure 6b). This small value is supported by the crystallographic data, which do not show chemical paths connecting rotated Co(II) ions in neighboring layers.

Discussion and Conclusions

First, in this discussion we follow the steps suggested by Kahn[21] to interpret magnetic data for high-spin octahedral Co(II) compounds. Later, we use a novel approach that fits together magnetization data and EPR results and provides a clearer understanding of the experimental results.

The simplest model, valid in the temperature range where the susceptibility data was obtained, is to assume that only the lowest Kramers' doublet is thermally populated. In that case the spin Hamiltonian is given by eq 1 and the powder susceptibility can be written as

$$\chi_M(T) = \frac{N g^2 \mu_B{}^2}{4 k_B T} + C' \qquad (2)$$

where C' is the temperature-independent contribution arising from the excited doublet.[21] Fitting eq 2 to the values of the susceptibility obtained from magnetization data at 1 kG, we

(37) Zarembowitch, J.; Kahn, O. *Inorg. Chem.* **1984**, *23*, 589−593.

obtain $g = 4.330(3)$ and $C' = 0.016(3)$ emu/mol. It is interesting to point out that assuming a Curie−Weiss behavior for the low-temperature magnetic susceptibility (see Figure S2 in Supporting Information), one obtains $J \sim -0.40$ cm^{-1} (antiferromagnetic), which is compatible with the range $0.25 < |J| < 1.2$ cm^{-1} obtained from EPR data through the incomplete collapse of the hyperfine interaction.

Under the same approximation we propose for the magnetization the Brillouin function behavior predicted for uncoupled spins $S' = {}^1/_2$.[25] Fitting the Brillouin function to the whole set of magnetization data in Figure 3a,b gives $g = 4.49$, which compares well to the mean square isotropic average of the g factor, $g = 4.45$, calculated from the EPR results in Table 3. The difference between the g value obtained from eq 2 and that obtained from the Brillouin function is large and not well understood within the spin $^1/_2$ model. Also, the observed increase of the magnetization at high fields cannot be followed by the calculated curves using the Brillouin function with $S' = {}^1/_2$ because the population of the excited spin doublet increases with T.

To obtain information about the zero-field splitting (ZFS) δ between the two spin doublets, we used the more elaborate model given by Kahn,[21] which takes into account the Zeeman energy, the ZFS, and the spin−orbit interaction for a high-spin Co(II) ion in octahedral surrounding with axial distortion. A basis set of 12 states associated with the $^4T_{1g}$ ground multiplet ($M_L = 0, \pm 1$ and $M_S = \pm {}^1/_2, \pm {}^3/_2$)) is considered in this model. It has four parameters, the splitting Δ between the $^4A_{2g}$ and ^4E_g of the $^4T_{1g}$ ground multiplet in D_{4h} symmetry, the spin−orbit coupling λ for the Co(II) ion, the parameter κ considering the mixing of the $^4T_{1g}$ states arising from the ground ^4F and the excited ^4P terms, and an isotropic g_0 factor appropriate for the ground term. We attempted without success to fit these four parameters to the magnetization data in Figure 3a,b. We attribute this failure to the neglect of rhombic distortions and to the inadequacy of the magnetization data to provide information about this large set of states.

Much better results were obtained considering only the two Kramers' doublets corresponding to a spin $S = {}^3/_2$, using the spin Hamiltonian,

$$\mathcal{H} = \mu_B \mathbf{S}\cdot\mathbf{g_0}\cdot\mathbf{H} + \mathbf{S}\cdot\mathbf{D}\cdot\mathbf{S} \qquad (3)$$

where **D** is a symmetric and traceless tensor and $\mathbf{g_0}$ is a **g** tensor defined over the $S = {}^3/_2$ quartet. We calculated the parameters of that spin Hamiltonian by a simultaneous global fit of eq 3 to the whole set of magnetization data in Figure 3a,b, and to the values of the three principal g factors of the ground doublet state obtained from the EPR experiments (Table 3). This global fit was performed with the simulated annealing method[26] and produces systematically an isotropic g_0 factor for the $S = {}^3/_2$ quartet. For an isotropic g_0, the **D** tensor is diagonal and eq 3 can be rewritten as[20,38]

$$\mathcal{H} = g_0\mu_B\mathbf{S}\cdot\mathbf{H} + D[S_z^2 - S(S+1)/3] + E(S_x^2 - S_y^2) \qquad (4)$$

where D and E are the axial and rhombic ZFS parameters, respectively. We obtained $g_0 = 2.60(1)$, $D = 114(4)$ cm^{-1}, and $E = -10(1)$ cm^{-1} where the uncertainties reflect the reproducibility of these results in different annealing processes.[27,28] These values for the spin Hamiltonian parameters within the $S = {}^3/_2$ quartet reproduce well the values of the magnetization (see solid lines in Figure 3a,b), and the values of the g factor of the ground doublet along the three principal directions (Table 3). The root-mean-square deviation of the result of this global fit from the magnetization data is ~3 times smaller than that obtained by fitting the Brillouin function for $S' = {}^1/_2$.

It is important to consider that the values of D and E are not unique.[38] They depend on the assignment of the three principal g factors of the ground doublet to the x, y, and z directions of the **D** tensor, and we chose these axes such that $|E| \leq |D/3|$. The ZFS parameter between the two spin doublets calculated with these values of D and E is $\delta = 2D[1 + 3(E/D)^2]^{1/2} \sim 231$ cm^{-1}. The value δ of the ZFS calculated from the fit follows the correlation coordination number/ZFS, which predicts ZFS > 50 cm^{-1} for six-coordinated Co(II) ions.[39,40] Since there is a sizable rhombic distortion (E term in eq 4), the ground and excited doublets cannot be assigned to either $\pm {}^1/_2$ or $\pm {}^3/_2$ doublets, as they are a mixture of them.

The g factors calculated for the lowest Kramers doublet with the results of the global fit are $g_x = 5.82$, $g_y = 4.50$, and $g_z = 2.54$, in good agreement with the experimental values in Table 3. In addition, the global fit shows that the smallest g value corresponds to the z direction of the Hamiltonian of eq 4. Globally fitting the spin Hamiltonian parameters to both magnetization and EPR data was important to ensure a single solution to the problem. We observed that fitting to only magnetization data does not give a single set of parameters. Difficulties to fit simultaneously EPR and magnetic results for high-spin Co(II) ions were reported by Adrait at al.[8] This problem has been solved in our work.

Fittings of a spin Hamiltonian for $S = {}^3/_2$ to magnetic data for high-spin cobalt compounds with octahedral coordination and six oxygen ligands have been reported by Matzapetakis et al.[41] and more recently by Jancovics et al.[42] Matzapetakis et al. obtained for a Co(II) citrate complex an isotropic g value $g_0 = 2.42$ and a very small ZFS $D = 0.83$ cm^{-1} assuming axial symmetry. Jancovics et al. studied a complex of Co(II) with imino-bis(methyl phosphonic acid). Assuming axial g factors and rhombic ZFS, they evaluated from susceptibility measurements $g_{0//} = 1.40$ and $g_{0\perp} = 2.53$ with $D = 52$ cm^{-1} and $E/D = 0.33$.

(38) Weil, J. A.; Bolton, J. R.; Wertz, J. E. *Electron Paramagnetic Resonance. Elementary Theory and Practical Applications*; Wiley: New York, 1994.
(39) Makinen, M. W.; Kuo, L. C.; Yim, M. B.; Wells, G. B.; Fukuyama, J. M.; Kim, J. E. *J. Am. Chem. Soc.* **1985**, *107*, 5245−5255.
(40) Larrabee, J. A.; Alessi, C. M.; Asiedu, E. T.; Cook, J. O.; Hoerning, K. R.; Klingler, L. J.; Okin, G. S.; Santee, S. G.; Volkert, T. L. *J. Am. Chem. Soc.* **1997**, *119*, 4182−4196 and references therein.
(41) Matzapetakis, M.; Dakanali, M.; Raptopoulou, C. P.; Tangoulis, V.; Terzis, A.; Moon, N.; Giapintzakis, J.; Salifoglou, A. *J. Biol. Inorg. Chem.* **2000**, *5*, 469−474.
(42) Jankovics, H.; Daskalakis, M.; Raptopoulou, C. P.; Terzis, A.; Tangoulis, V.; Giapintzakis, J.; Kiss, T.; Salifoglou, A. *Inorg. Chem.* **2002**, *41*, 3366−3374.

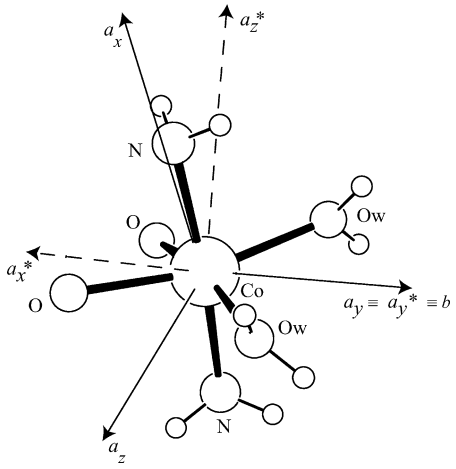

Figure 7. The two possible orientations of the principal axes of the **g** tensor for the Co(II) site.

Our EPR results provide the eigenvectors of the **g** tensor of the ground doublet. The two rotated Co(II) sites in the unit cell introduce an intrinsic limitation to assigning the eigenvectors of the **g** tensor to one particular site. The two possible assignments, a_x, a_y, a_z and a_x*, a_y*, a_z*, are given in Table 3 and are displayed in Figure 7. Table 3 also includes the angles between the principal axes a_x and a_z* and the Co−N bond for each assignment. The solid arrows in Figure 7 correspond to a situation where the principal direction a_x is close to the Co−N bond, the principal direction a_y is bisecting the Co−O bonds, and the direction a_z is approximately bisecting the Co−O bonds. The dashed arrows correspond to a situation where none of the principal directions of the **g** tensor (a_x*, a_y*, a_z*) are along a bond direction. There is not much work performed on low-symmetry high-spin octahedral cobalt systems regarding the assignment of the **g** tensor axes with the molecular structure of the metal site; previous works were performed on systems having different metal site coordination, which does not allow a clear comparison.[43] We favor the choice a_x, a_y, a_z with one eigenvector along the Co−N bond, which is perpendicular to the C_2 symmetry *b* axis of the metal site. However, theoretical work should be performed about this point.

In conclusion, our structural and magnetic study of Co(L-Thr)$_2$ indicates high-spin Co(II) ions in a distorted octahedral ligand field, arranged in layers. EPR data provides information about the absolute values of the intralayer and interlayer interactions J and J'. We explain the observed incomplete collapse of the hyperfine structure proposing $0.25 < |J| < 1.2$ cm^{-1} for the interaction between Co(II) neighbors in a layer. The weaker interaction between Co(II) ions in neighboring layers was estimated to be $|J'| < 0.07$ cm^{-1}. The **g** values corresponding to the ground doublet obtained from the EPR spectra agree with those found from magnetization data. A global fit of the magnetization and EPR results with a $S = {}^3/_2$ spin Hamiltonian allowed us to calculate a ZFS $\delta \sim 231$ cm^{-1} between ground and excited doublets.

Acknowledgment. We thank M. Perec for valuable discussions and help on the characterization of the complex; we are also grateful to L. Ghivelder for help during the magnetic measurements. This work was supported by CONICET and CAI+D-UNL in Argentina and CNPq and FAPERJ in Brazil. Multinational grants of Antorchas and Andes Foundations made possible this collaboration. R.C. is a fellow of CONICET.

Supporting Information Available: Listing of data collection and structure refinement methods (Table S1), atomic coordinates and equivalent isotropic displacement parameters (Table S2), bond lengths and angles (Table S3), anisotropic displacement parameters (Table S4), hydrogen coordinates and isotropic displacement parameters (Table S5), a plot showing the H-bonds supporting the Co−Co interactions within a layer (Figure S1), and Curie plot of the molar magnetic susceptibility vs temperature data (Figure S2). This material is available free of charge via the Internet at http://pubs.acs.org.

IC026111B

(43) Bencini, A.; Gatteschi, D. *Inorg. Chem.* **1977**, *16*, 2141−2142. Bencini, A.; Benelli, C.; Gatteschi, D.; Zanchini, C. *Inorg. Chem.* **1979**, *18*, 2526−2528; **1979**, *18*, 2137−2140.